http://dx.doi.org/10.5935/0103-5053.20150184

J. Braz. Chem. Soc., Vol. 26, No. 10, 2035-2045, 2015.
Printed in Brazil - ©2015 Sociedade Brasileira de Química
0103 - 5053 $6.00+0.00

Article

Development of a Selective and Sensitive Sensor for Urate Determination Based on Tris(1,10-phenantroline)copper(II) Bis(tetracyanoquinodimethanide) Adsorbed on Carbon Nanotubes

Dilton M. Pimentel,[a] Fernando M. de Oliveira,[a] Wallans T. P. dos Santos,[b] Lauro T. Kubota,[c] Flávio S. Damos[d] and Rita C. S. Luz*[,d]

[a]*Departamento de Química and* [b]*Departamento de Farmácia, Universidade Federal dos Vales do Jequitinhonha e Mucuri (UFVJM), Rodovia MGT 367, km 583, No. 5000, Alto da Jacuba, 39100-000 Diamantina-MG, Brazil*

[c]*Departamento de Química Analítica, Instituto de Química, Universidade Estadual de Campinas (Unicamp), P.O. Box 6154, 13083-970 Campinas-SP, Brazil*

[d]*Departamento de Química, Universidade Federal do Maranhão (UFMA), Avenida dos Portugueses, s/n, Bacanga, 65080-805 São Luís-MA, Brazil*

The present work describes the development of a selective electrochemical sensor for urate based on tris(1,10-phenantroline)copper(II) bis(tetracyanoquinodimethanide) ($Cu(phen)_3(TCNQ)_2$) adsorbed on multi-walled carbon nanotubes (CNT). The composite material was characterized by infrared spectroscopy, scanning electron microscopy, and electrochemical impedance spectroscopy. The composite material showed an excellent electrocatalytic activity toward oxidation of urate. The heterogeneous charge transfer rate constant (k') between the analyte and the sensor was determined using linear sweep voltammetry experiments. The composite material shows a linear range from 5 up to 2500 μmol L^{-1} with limit of detection of 1.05 μmol L^{-1} and limit of quantification of 3.50 μmol L^{-1}. The high sensitivity and selectivity of the sensor for urate was sufficient for its determination in biological fluids. Finally, the proposed sensor was successfully applied in urine samples.

Keywords: $Cu(phen)_3(TCNQ)_2$, functionalized carbon nanotubes, urate

Introduction

Urate (UA) is an important biological compound from purine's metabolism, it has a hole of selective antioxidant, capable of reaction with hydroxyl radicals and hypochlorous acid.[1] Usually, its normal level in urinary excretion is in the concentration range 1.49-4.46 mmol L^{-1},[2] while in blood it is 0.15-0.45 mmol L^{-1}.[3] Anomalous levels of UA can be associated with many sicknesses such as hyperuricemia,[4] gout,[5] Lesch-Nyhan syndrome[6] and Parkinson's disease.[7,8] In this sense, the development of a sensitive, selective and fast method for UA determination is highly important to collaborate with the diagnostic of aforementioned diseases. With this goal, many techniques are applied to urate determination including fluorescence,[3] electrochemiluminescence,[2] capillary electrophoresis with contactless conductivity,[9] high-performance liquid chromatography (HPLC) linked with mass spectrometry,[10] and many others. Among the used techniques, the electrochemical methods show some advantages like relative low cost, quickness and very low limits of quantification. However, the common issue in voltammetric measurements regards the overlapping of responses due to UA, ascorbate (AA) and adrenaline (AD), oxidations which occur at adjacent potentials. This issue can be resolved by the development of selective and sensitive composite materials.[11,12]

Charge transfer complexes based on 7,7,8,8-tetracyanoquinodimethane (TCNQ) have been intensively studied due to its rich array of electrical, electrochemical, optical, and spectroscopic properties. This is particularly true where these compounds take the form of nanoparticles, micro- and nano-rod crystals, thin films, or self-assembled monolayers on a substrate that may be incorporated into a device for energy or information storage, catalysis, or sensing applications.

*e-mail: rita.luz@ufma.br

$M_x^+[TCNQ]_x^-$ derivatives (designated below as MTCNQ, M = transition metal) have also been synthesized and characterized. Frequently, these metal complexes behave as organic semiconductors, some of which may be used as mediators or electrocatalysts, as in the case with ($Cu(phen)_3(TCNQ)_2$).[13-15]

There are numerous advantages in investigating this type of material, as synthesis is straightforward and properties, such as conductivity, can be controlled systematically by either changing the metal cation or the electron acceptor. The bonding arrangement between the central cation and the anions can also be varied, with the copper-TCNQ complexes being of particular interest, as they can exist as both a kinetically and thermodynamically stable phase with significantly different conductivities.[16] This is due to differences in the stacking arrangement of the interpenetrating networks of TCNQ within the structures, where the phase I shows efficient p-stacking, and hence higher conductivity, compared to phase II which does not, due to the larger distance between the individual TCNQ layers.[16]

However, the modifications that consist only of TCNQ are not stable enough and researches showed that more efficient modifications can be obtained by the association with other materials.[17] A number of methods have been developed to acquire and stabilize copper-TCNQ crystals in its conducting phase I. In recent years, several research groups have demonstrated that composites based on charge transfer complexes based on TCNQ and multi-walled carbon nanotubes (CNT) can form supramolecular arrangement due to π-π interactions.[18] Indeed, CNT has been exploited to promote high-quality nano- and microwires of charge transfer complexes based on TCNQ.[19]

In this sense, the present work reports the development of an efficient and stable sensor based on CNT functionalized with the compound tris(1,10-phenantroline)copper(II) bis(tetracyanoquinodimethanide) for sensitive, stable and selective determination of urate in urine samples.

Experimental

Reagents and solutions

All chemicals were of analytical grade and were used as received without further purification. The multi-walled carbon nanotubes (CNT, > 90% purity, 110-170 nm diameter, 5-9 μm length) was purchased from Sigma-Aldrich®. UA was purchased from Proquímios. 1,10-Phenanthroline hydrochloride monohydrate was acquired from Riedel-de-Haën. 7,7,8,8-Tetracyanoquinodimethane and acetonitrile were acquired from Acros Organics and lithium iodide was acquired from Merck. The synthesis and characterization of $Cu(phen)_3(TCNQ)_2$ was performed according to literature.[20,21] Tris(hydroxymethyl)aminomethane (Tris), hydrochloric acid, sodium hydroxide and monosodium phosphate were purchased from Vetec.

All solutions were prepared with water purified in a Milli-Q Millipore system PURELAB Classic DI Belga (resistivity > 18 MΩ) and the actual pH of the buffer solutions was determined with a Digimed DM-20 pHmeter.

Material characterization and electrochemical measurements

The scanning electron microscopy (SEM) measurements were performed using a Shimadzu VEGA 3 TESCAN scanning electron microscope. The Fourier transform infrared spectroscopy (FTIR) was carried out with a FT-IR VARIAN 640 IR spectrometer.

The cyclic voltammetry (CV) and differential pulse voltammetry (DPV) were performed with a potentiostat/galvanostat model PGSTAT 101 from Autolab coupled to a microcomputer with NOVA 1.7 software. The electrochemical impedance spectroscopy (EIS) measurements were performed with a PGSTAT 128 N potentiostat/galvanostat from Autolab coupled to a microcomputer with GPES and FRA 4.9 software. The hydrodynamic measurements were carried out with a motor rotation from PINE Instruments. The electrochemical cell was a conventional three electrodes cell containing Ag/AgCl(sat.) as reference electrode, a gold wire as auxiliary electrode and a glassy carbon electrode (GCE) (bare or modified) as work electrode.

Carbon nanotubes functionalization

The CNT were functionalized preparing a dispersion containing 50 mg of CNT and 6 mg of $Cu(phen)_3(TCNQ)_2$ in 10 mL of dimethylsulfoxide (DMSO) which was maintained at rest and room temperature for 72 h. Then, the prepared dispersion was filtered under vacuum. The obtained material ($Cu(phen)_3(TCNQ)_2$/CNT) was dried at 40 °C and used to prepare an aqueous dispersion for later modification of electrode surface.

Preparation of modified electrode

The GCE was polished with alumina powder before its modification. A volume of 5 μL of the dispersion of $Cu(phen)_3(TCNQ)_2$/CNT was dropped on the GCE surface and it was allowed to dry at 40 °C for 15 min. After this step, the modified electrode $Cu(phen)_3(TCNQ)_2$/CNT/GCE

was thoroughly rinsed with distilled water. Control experiments were also carried out with bare GCE, GCE modified with a CNT dispersion and GCE modified with $Cu(phen)_3(TCNQ)_2$.

Results and Discussion

Characterization of the $Cu(phen)_3(TCNQ)_2$/CNT composite material

The morphologies of CNT, $Cu(phen)_3(TCNQ)_2$, and $Cu(phen)_3(TCNQ)_2$/CNT composite were investigated by SEM and the results are presented in Figures 1A-C. The SEM images of CNT and $Cu(phen)_3(TCNQ)_2$ complex are depicted in Figures 1A and 1B, respectively. As can be seen in Figure 1B, $Cu(phen)_3(TCNQ)_2$ shows a layered structure consisting of well packed sheets over the surface. This kind of morphology is usual for the phase II of metal-TCNQ charge transfer complexes.[22]

On the other hand, Figure 1C reveals the presence of microrods of $Cu(phen)_3(TCNQ)_2$ with a diameter of about 2 μm and a length of 15 μm (approximately) embedded in the CNT structure. We believe that the nucleation and growth of microrods of $Cu(phen)_3(TCNQ)_2$ in the CNT structure is favored due to the strong interaction between CNT with the charge transfer complex.[19]

The chemical composition of unmodified CNT, $Cu(phen)_3(TCNQ)_2$ and $Cu(phen)_3(TCNQ)_2$/CNT surfaces were characterized by FTIR (Figure 1D, spectra a-c). The FTIR spectrum of the unmodified CNT (Figure 1D, spectrum a) shows a broad C–H alkyl stretching peak at 2850-3000 cm^{-1}, a sharp C=O stretching peak from the

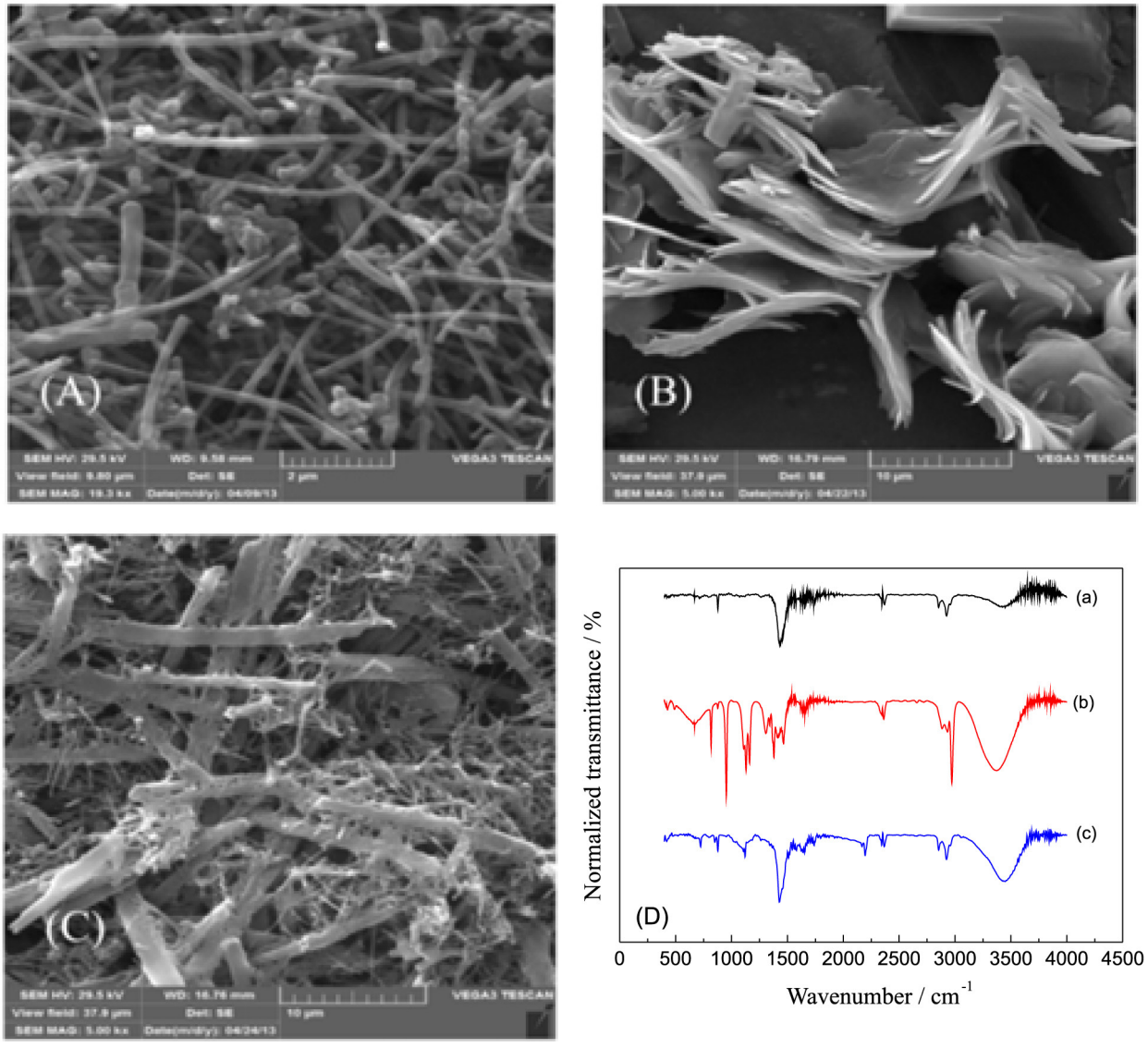

Figure 1. SEM images of (A) CNT, (B) $Cu(phen)_3(TCNQ)_2$, (C) $Cu(phen)_3(TCNQ)_2$/CNT and (D) FTIR spectra of (a, black curve) CNT, (b, red curve) $Cu(phen)_3(TCNQ)_2$ and (c, blue curve) $Cu(phen)_3(TCNQ)_2$/CNT.

COOH groups at 1450 cm^{-1} and a broad O–H stretching peak between 3400 and 3600 cm^{-1}.

The IR values, ν(C–H), 835 and 723 cm^{-1} observed for phenanthroline are red shifted to 865 and 800 cm^{-1}. These red shifts can be explained by the fact that each of the two nitrogen atoms of phenanthroline ligands donates a pair of electrons to the central metal forming a coordinate covalent bond.[23] Ring stretching frequencies ν(C=C) and ν(C=N) at 1519 and 1444 cm^{-1} for free phenantroline shift to higher frequencies upon complexation, indicating coordination of the heterocyclic nitrogen. Absorptions at 420-493 cm^{-1} are ascribed to the formation of Cu–N bonds, respectively.[24] The complex displays an intense and broad band centered at 3400 cm^{-1} that can be assigned to O–H stretching vibration of the water molecules and the broadness is indicative of hydrogen bonds.

The FTIR spectrum of the composite $Cu(phen)_3(TCNQ)_2$/CNT (Figure 1D, spectrum c) confirms the modification of CNT through the presence of the characteristic bands of both compounds shown in Figure 1D, spectra a and b. In addition, the FTIR spectrum obtained for $Cu(phen)_3(TCNQ)_2$/CNT composite shows a band at 2200 cm^{-1} associated with phase I of copper-TCNQ complexes.[25]

Electrochemical behavior of $Cu(phen)_3(TCNQ)_2$/CNT/GCE

After modifying the electrode with the $Cu(phen)_3(TCNQ)_2$/CNT composite, 20 cycles were scanned in the potential range from –0.8 to 0.8 V in 0.1 mol L^{-1} phosphate buffer solution (PBS) at a scan rate of 0.05 V s^{-1} (Figure 2). $Cu(phen)_3(TCNQ)_2$/CNT/GCE provided a stable electrochemical response. As can be seen in Figure 2, the cyclic voltammograms exhibit two anodic peaks at forward scan of potential and two cathodic peaks in backward scan of the potential.

$Cu(phen)_3(TCNQ)_2$/CNT/GCE displays an initial $TCNQ^{0/\bullet-}$ reduction process (Figure 2, labelled as process 1) with 1_{red} and 1_{ox} being associated with TCNQ reduction and $TCNQ^{\bullet-}$ oxidation, respectively. A number of copper-TCNQ modified electrodes show the presence of a symmetrical peak on switching the scan direction to more positive values. This behavior has been associated with partial stripping of copper-TCNQ when the potential is returned to more positive values.[25]

However, the cyclic voltammograms (CVs) for $Cu(phen)_3(TCNQ)_2$/CNT/GCE do not show a symmetric redox peak due to the stripping of the $Cu(phen)_3(TCNQ)_2$ complex. It is probable that the composite becomes constituted by more strongly adhered crystals on the electrode surface, which are more difficult to strip from the electrode surface.[26] As a consequence, after 20 cycles

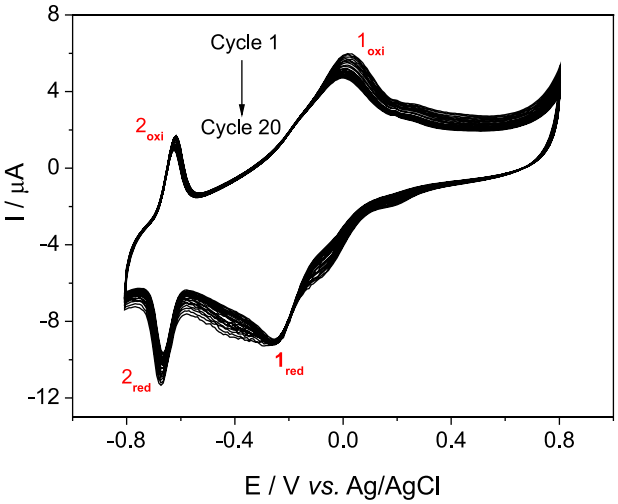

Figure 2. Cyclic voltammograms of $Cu(phen)_3(TCNQ)_2$/CNT/GCE in 0.1 mol L^{-1} PBS. Scan rate: 50 mV s^{-1}.

the relative standard deviation (RSD) was lower than 2% for the last 5 cycles indicating a good stability. Finally, at more negative potentials a redox couple is detected (labelled as process 2 in Figure 2) with very sharp, symmetrical reduction (2_{red}) and oxidation (2_{ox}) peaks. According to the above results, and combining with the reaction mechanism which have been studied in previous reports,[25] the possible reaction mechanisms are summarized in the following equations:

Process 1 (redox couple 1)

$$2TCNQ + 2e^- \rightleftharpoons 2TCNQ^{\bullet-} \quad (1a)$$

$$2TCNQ^{\bullet-} + [Cu(phen)_3]^{2+} \rightleftharpoons Cu(phen)_3(TCNQ)_2 \quad (1b)$$

Process 2 (redox couple 2)

$$TCNQ + TCNQ^{\bullet-} + [Cu(phen)_3]^{2+} \rightleftharpoons Cu(phen)_3[(TCNQ)(TCNQ^{\bullet-})]^+ \quad (2a)$$

$$Cu(phen)_3[(TCNQ)(TCNQ^{\bullet-})]^+ + 1e^- \rightleftharpoons Cu(phen)_3(TCNQ)_2 \quad (2b)$$

In order to take information of the composite electrode kinetics, the difference between the peak potential (E_p) and the formal potential ($E^{0'}$) was evaluated as a function of the logarithm of the scan rate (Figure 3). The results show that at high scan rate values the value of ΔE ($\Delta E = E_p - E^{0'}$) was higher than 200 mV. Therefore, the electron transfer coefficient (α) and the apparent heterogeneous rate constant of charge transfer (k_s) between the electrode and a surface-confined redox couple were estimated by method of Laviron.[27] The calculation of $E^{0'}$ was accomplished in conforming to the following equation (considering α ca. 0.5):[28]

$$E^{0'} = E_{p,a} - \alpha(E_{p,a} - E_{p,c}) \quad (3)$$

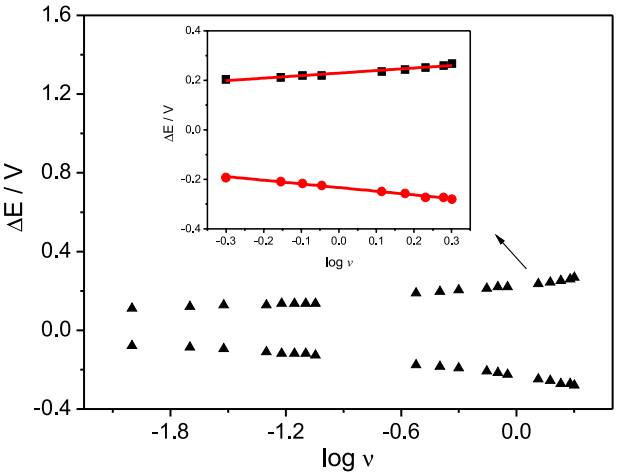

Figure 3. Relationship between ΔE and log ν for $Cu(phen)_3(TCNQ)_2$/CNT/GCE. Inset: plot of ΔE *vs.* log ν for $Cu(phen)_3(TCNQ)_2$/CNT/GCE at higher values of ν.

According to Laviron theory,[27] for high values of scan rates, the slope of the linear region of the plot of ΔE *vs.* ln ν (Figure 3) is equal to 2.303RT / α_anF for the anodic peak and –2.303RT / α_cnF for the cathodic peak. In this sense, the values 0.58 and 0.41 were obtained for α_a and α_c, respectively. Thus, the average 0.5 for α was used for determination of k_s according to the following equation:[27]

$$\log k_s = \alpha\log(1-\alpha) + (1-\alpha)\log\alpha - \log\left(\frac{RT}{nF\nu}\right) - \alpha(1-\alpha)nF\left(\frac{\Delta E}{2.3RT}\right) \quad (4)$$

where ν is the scan rate, n is the number of involved electrons, T is the temperature, R is the gas constant, F is the Faraday constant and all other symbols have the aforementioned meanings. The value found for k_s was 2.9 s^{-1}.

The electrode effective area, A, and the surface concentration of electroactive species, Γ, were also estimated. Initially, CVs in 1 mmol L^{-1} of $Fe(CN)_6^{3-}/Fe(CN)_6^{4-}$ (0.1 mol L^{-1} KCl) were performed at several rate scan values. The slope of the plot of current *vs.* square root of scan rate ($\nu^{1/2}$) and the Randles-Sevick equation[29] make it possible to get value of A:

$$i_p = (2.69\times10^5)n^{3/2}AD^{1/2}C^*\nu^{1/2}\ (T = 25\ ^\circ C) \quad (5)$$

where i_p is the peak current, n is the number of involved electrons, A is the electrode area, D is the diffusion coefficient of electroactive species, C* is the bulk concentration of electroactive species and ν the scan rate. The calculated area of the composite modified electrode was 0.092 cm^2 whereas the geometric area is 0.032 cm^2 contributing with the sensitivity of system. After this step, Γ value was estimated by using equation 6[30] and the value obtained was 2.89×10^{-9} mol cm^{-2}. The electrical charge Q was calculated by integration of peak current on the last cyclic voltammogram to the composite modified electrode.

$$\Gamma = \frac{Q}{nFA} \quad (6)$$

In addition, the electrochemical properties of $Cu(phen)_3(TCNQ)_2$/CNT/GCE were also verified by EIS using the redox couple $Fe(CN)_6^{3-}/Fe(CN)_6^{4-}$ (1 mmol L^{-1}) in aqueous solution of KCl (0.1 mol L^{-1}). This modification was evaluated in comparison with bare electrode and the other control experiments (GCE modified with CNT or $Cu(phen)_3(TCNQ)_2$) by Nyquist plot (Figure 4).

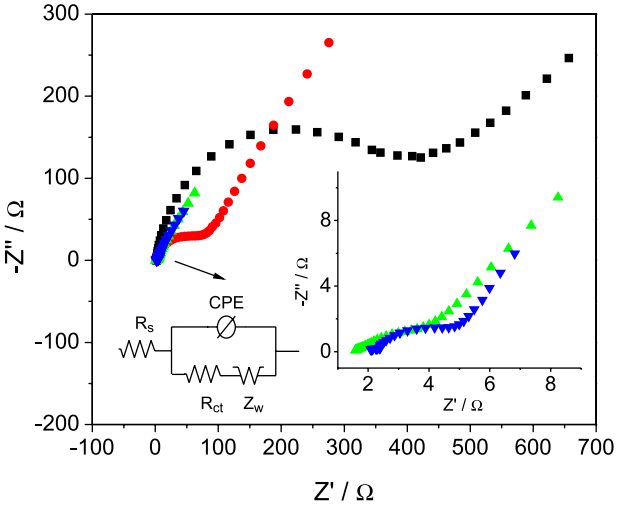

Figure 4. Nyquist plots for: bare GCE (black square), $Cu(phen)_3(TCNQ)_2$/GCE (red circle), CNT/GCE (green triangle) and $Cu(phen)_3(TCNQ)_2$/CNT/GCE (blue inverted triangle); Inset: magnification of the Nyquist plot for CNT/GCE and $Cu(phen)_3(TCNQ)_2$/CNT/GCE and the equivalent circuit for the purpose system. The measurements were performed with potassium ferricyanide (1 mmol L^{-1}) in 0.1 mol L^{-1} KCl.

The impedance spectra were fitted interpreting the electrochemical cell as a modified Randles equivalent electrical circuit, including the solution resistance (R_s) in series with a constant phase element (CPE) that is in parallel with the charge-transfer resistance (R_{ct}), which in turn is in series with Warburg impedance (Z_W) (Figure 4 inset). The CPE was used with the aim of considering the frequency dispersion of capacitance owing to atomic scale in homogeneity, porous geometry and roughness.[31]

The results show that the charge-transfer resistances of all modified electrodes ($Cu(phen)_3(TCNQ)_2$/GCE, CNT/GCE and $Cu(phen)_3(TCNQ)_2$/CNT/GCE, with charge transfer resistance of 78.8, 4.0 and 4.7 Ω, respectively) are much smaller than R_{ct} of bare electrode (410.0 Ω).

The CNT was responsible for the smallest R_{ct} observed justifying its application. The composite modified electrode showed a charge transfer resistance a little higher than the CNT/GCE, which possibly happens because of the synergistic effect between CNT and the ions $TCNQ^{-}$ and $Cu(phen)_3^{2+}$ (π-stacking). Nevertheless, the subsequent analyses show $Cu(phen)_3(TCNQ)_2$/CNT/GCE is more suitable than CNT/GCE for our analytical purpose.

Electrooxidation of UA and AD in presence of AA on $Cu(phen)_3(TCNQ)_2$/CNT/GCE and effects of the experimental conditions

$Cu(phen)_3(TCNQ)_2$/CNT/GCE was tested in presence of AA, AD and UA and analyzed in comparison with other modifications (Figure 5). As can be seen in Figures 5a-d, the peak potentials for AA, AD and UA are superimposed at bare GCE (a), CNT/GCE (b), and $Cu(phen)_3(TCNQ)_2$/GCE (c). Figures 5a and 5b show that it is impossible to determine the individual concentration of these compounds from the merged voltammetric peaks. On the other hand, the use of CNT/GCE (Figure 5c) and $Cu(phen)_3(TCNQ)_2$/CNT/GCE (Figure 5d) were selective to AA, AD and UA. However, $Cu(phen)_3(TCNQ)_2$/CNT/GCE showed higher peak current to AA, AD, and UA than that on CNT/GCE (Figure 5d). Thus, $Cu(phen)_3(TCNQ)_2$/CNT/GCE is a feasible method for selective and sensitive oxidation of AA, AD and UA due to the ability of CNT in fixing and controlling the stability and electrochemical performance of the $Cu(phen)_3(TCNQ)_2$ charge transfer complex.[32] The following mechanisms can be proposed for oxidation of the analytes on the $Cu(phen)_3(TCNQ)_2$/CNT modified electrode:

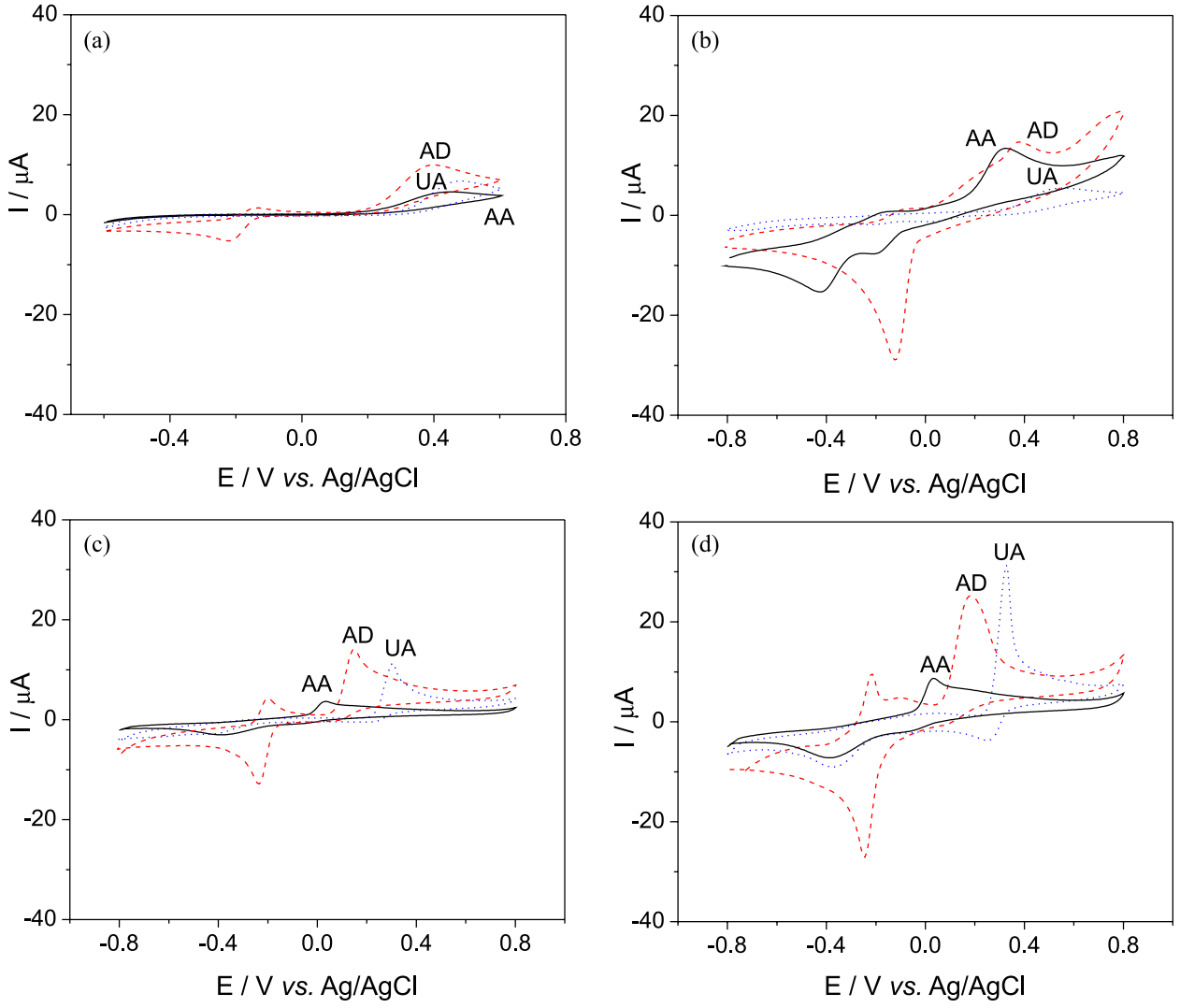

Figure 5. Cyclic voltammograms of AA (black curve), AD (red curve) or UA (blue curve) on (a) bare GCE, (b) $Cu(phen)_3(TCNQ)_2$/GCE, (c) CNT/GCE and (d) $Cu(phen)_3(TCNQ)_2$/CNT/GCE. Experiments carried out in 0.1 mol L^{-1} PBS (pH 7.0) and v = 50 mV s^{-1}.

$$Cu(phen)_3(TCNQ)_2 - 1e^- \rightleftharpoons Cu(phen)_3[(TCNQ)(TCNQ)^-)]^+ \quad (7)$$

$$Cu(phen)_3[(TCNQ)(TCNQ)^-)]^+ + analyte_{(reduced\ form)} \rightleftharpoons Cu(phen)_3(TCNQ)_2 + analyte_{(oxidized\ form)} \quad (8)$$

The influence of $Cu(phen)_3(TCNQ)_2$ concentration for functionalization of nanotubes was evaluated preparing five solutions in DMSO (0.2, 0.4, 0.6, 0.8 and 1.0 mg mL^{-1}) and modifying the electrode with the composites obtained. The best result (higher sensitivity toward AA, AD and UA oxidation) was acquired using 0.6 mg mL^{-1} which was utilized in subsequent analysis. The less concentrated solutions are probably not able to adsorb sufficient electrocatalytic species on CNT structure. On the other hand, more concentrated ones may change dramatically the network of sp^2 carbons from nanotubes hampering the charge transfer.

The concentration of the CNT dispersion for GCE modification was also studied (1.0, 2.0, 3.0, 4.0 and 5.0 mg mL^{-1}) always dropping 5 µL on electrode surface. The best result was observed with 3.0 mg mL^{-1}. The concentration is related to surface coverage, thus low concentrations cannot entirely cover the electrode. Notwithstanding, the higher concentrations of CNT can generate thick covers that are instable and not further the charge transfer. Lastly, the nature and pH (6.0, 6.5, 7.0, 7.5, 8.0 and 8.5) of buffer was chosen by comparing the 0.1 mol L^{-1} McIlvaine, Hepes, Tris and PBS solutions. The highest peak currents were observed using PBS between pH 7.0 and 7.5 (data not shown).

Urate oxidation on $Cu(phen)_3(TCNQ)_2$/CNT/GCE

The number of electrons involved in the electrochemical reaction of UA on the composite modified electrode was estimated by plotting the peak current *vs.* square root of scan rate, which displayed a linear relationship (Figure 6a), indicating a mass transport limitation. For irreversible behavior the equation 9 can be applied:[33]

$$i_p = (2.99 \times 10^5)(\alpha_a n_a)^{1/2} nAC^* D^{1/2} v^{1/2} \quad (9)$$

where n_a is the number of electrons involved in the rate-determining step and all other symbols have the meanings aforementioned.

Considering the necessary knowledge of the $(\alpha_a n_a)$ value presented in equation 9, one approach was employed, based on the shift of the peak potential as a function of scan rate.[33] In this sense, based on the simplified expression for an irreversible reaction, the change in E_{pa} for each 10-fold increase in v is 1.15RT / $[\alpha_a n_a]$F,[33] the plot of E_{pa} *vs.* log v indicates a linear variation with the values of $[\alpha_a n_a]$ estimated as being 1.44. Thus, using the value of $[\alpha_a n_a]$ in equation 9 and the slope of inset of Figure 6a, the value of n was

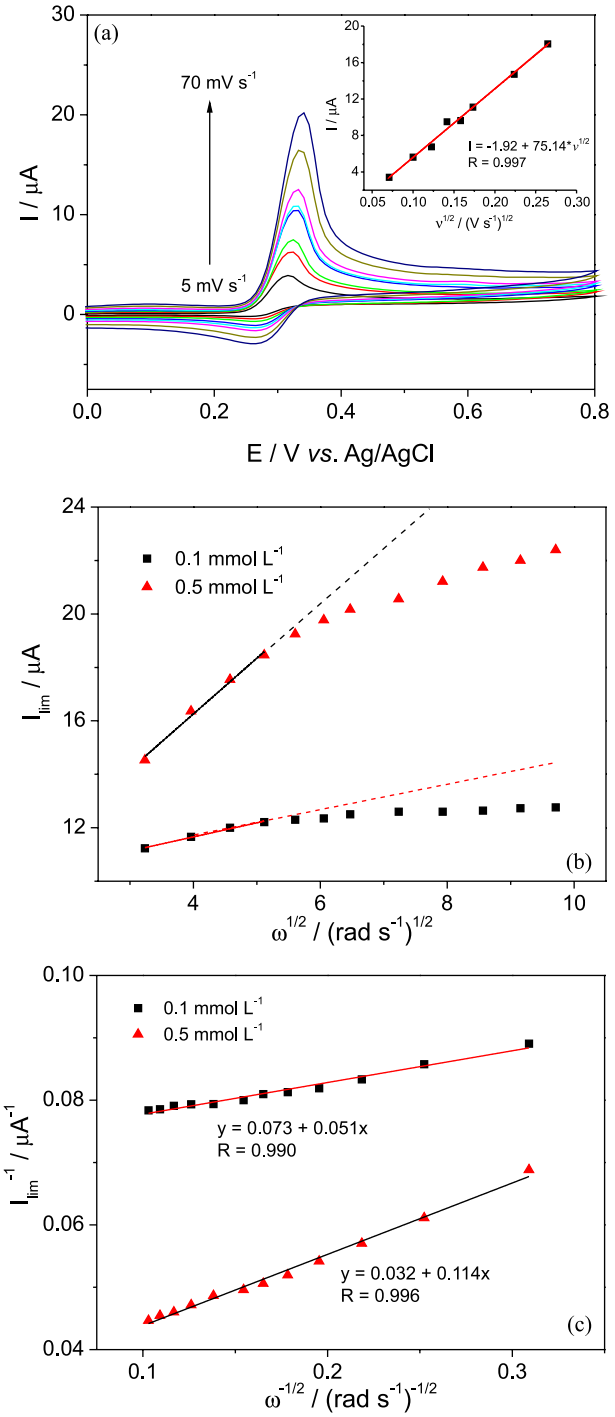

Figure 6. (a) Cyclic voltammograms for $Cu(phen)_3(TCNQ)_2$/CNT/GCE in presence of 0.5 mmol L^{-1} UA in 0.1 mol L^{-1} PBS (pH 7.0). The scan rate was shifted according to the values 5; 10; 15; 20; 25; 30; 50 and 70 mV s^{-1}. Inset: linear relationship between I_p and $v^{1/2}$; (b) Levich plot obtained from hydrodynamic voltammograms of $Cu(phen)_3(TCNQ)_2$/CNT/GCE for solutions of 0.1 mmol L^{-1} (square) and 0.5 mmol L^{-1} (triangle) UA in 0.1 mol L^{-1} PBS (pH 7.0); (c) Koutecky-Levich plots constructed from Levich plots shown in (b).

calculated to be 2.02, suggesting a transfer mechanism of 2 electrons for the electrocatalytic oxidation of UA. This result is in agreement with the works reported in the literature based on the catalytic oxidation of UA.[34] The diffusion coefficient considered was 5.1×10^{-6} cm^2 s^{-1} for UA.[35]

In order to take more information about UA oxidation on the composite material, hydrodynamic measurements were also performed. In this sense, polarization curves for UA oxidation reaction recorded at several electrode rotation rates ω (100, 150, 200, 250, 300, 350, 400, 500, 600, 700, 800 and 900 rpm) and different UA concentrations (0.1 and 0.5 mmol L^{-1}) in PBS (pH 7.0) with a potential scan rate of 0.01 V s^{-1} were performed. The limiting currents (I_{lim}) obtained for the modified electrode increase with the rotation speed. The linearity of the Levich plots observed at lower rotation rates indicates that the reaction is controlled by mass transport. On the other hand, a deviation of the linearity in the Levich plots observed at higher rotation rates suggests a kinetic limitation (Figure 6b). For higher values of rotation rate, the thickness of the Levich layer decreases and the magnitude of the current begins to be controlled by the rate of the redox mediated reaction between UA and composite. In this case, the polarization curves are more conveniently analyzed by means of Koutecky-Levich plots (Figure 6c), where the currents for UA oxidation on the rotating disk electrode are analyzed in potential regions where the mass transport and kinetic contributions are related as follows:[29]

$$\frac{1}{I_{lim}} = \frac{1}{I_{Lev}} + \frac{1}{I_k} = \frac{1}{0.62nFAD^{2/3}v_k^{-1/6}\omega^{1/2}C} + \frac{1}{nFACk_{obs}\Gamma} \quad (10)$$

in this case v_k represents the kinematic viscosity, I_{Lev} the current limited by mass transport and all other symbols have the meanings aforementioned.

The values of k_{obs} decreased from 2.67×10^6 to 1.18×10^6 cm^3 mol^{-1} s^{-1} as the bulk concentration of UA increased from 0.1 to 0.5 mmol L^{-1}. From the slope and intercept of the plot k_{obs} *vs.* [UA] a straight line was obtained and the extrapolated value of k_{obs} to zero UA concentration was estimated as 3.04×10^6 cm^3 mol^{-1} s^{-1}. Take into account that $k' = k_{obs} \times \Gamma$, that is the rate constant considering the surface concentration of electroactive species, the value of 8.79×10^{-3} cm s^{-1} was calculated. The k' value is higher than other reported in literature for reaction between UA and chemically modified electrodes.[35-39]

Resolution of peaks and analytical characterization

The selective UA oxidation on $Cu(phen)_3(TCNQ)_2$/CNT/GCE was evaluated by DPV keeping constant the AD (100 μmol L^{-1}) and AA (50 μmol L^{-1}) concentration while changing UA concentration in the range of 45 up to 135 μmol L^{-1} (Figure 7a). The linear behavior of the UA response (inset of Figure 7a) was not affected in presence of AD and AA showing that the proposed electrode can be used in samples containing these foreign species.

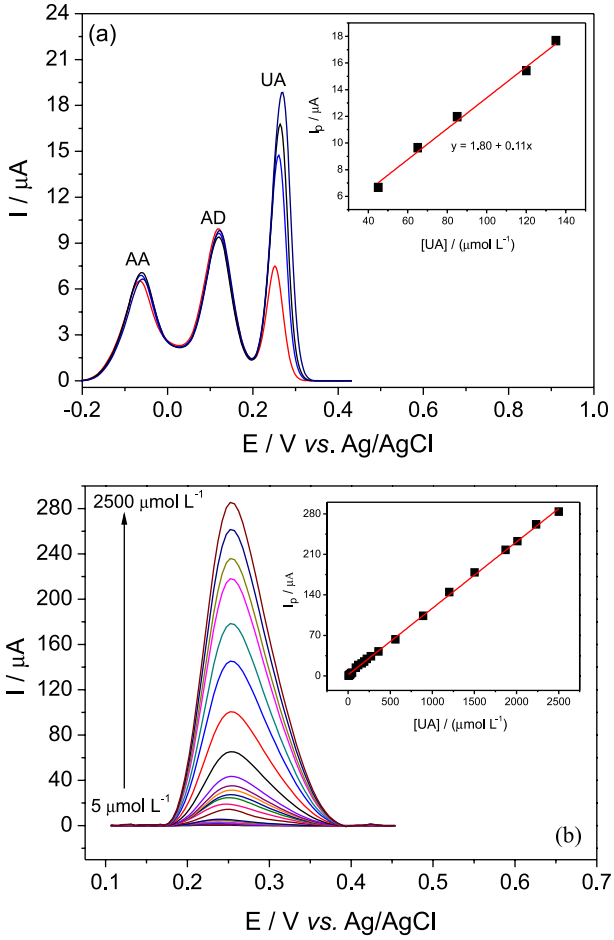

Figure 7. (a) DPV of $Cu(phen)_3(TCNQ)_2$/CNT/GCE in 0.1 mol L^{-1} PBS (pH 7.0) containing 50.0 μmol L^{-1} AA and 100.0 μmol L^{-1} AD and different concentrations of UA: 45.0, 65.0, 100.0, 120.0 and 135.0 μmol L^{-1}. Inset: linear relationship between the peak current and [UA]. v = 60 mV s^{-1}; amplitude = 140 mV. (b) DPV of $Cu(phen)_3(TCNQ)_2$/CNT/GCE in 0.1 mol L^{-1} PBS (pH 7.0) containing different concentrations of UA: 5.0-2500 μmol L^{-1}. Inset: analytical curve constructed. v = 60 mV s^{-1}; amplitude = 140 mV.

Figure 7b shows the DPV recorded for $Cu(phen)_3(TCNQ)_2$/CNT/GCE in successive additions of UA into the PBS. Inset of Figure 7b shows the analytical curve for UA. A wide linear response range from 5 up to 2500 μmol L^{-1} was observed, which can be expressed according to the equation:

$$I_p\ (\mu A) = 0.01 + 0.11\ [UA]\ (\mu mol\ L^{-1}) \quad (11)$$

with a correlation coefficient of 0.998. The sensitivity and the linear range were as good as or even better when

compared with many works reported in the literature (Table 1).[36-45] Such good sensitivity can be attributed to the efficiency of the electron transfer between $Cu(phen)_3(TCNQ)_2$/CNT modified electrode and UA, favored by highly dispersed $Cu(phen)_3(TCNQ)_2$ complex on the CNT. The limits of detection and quantification were estimated as 1.05 and 3.50 μmol L^{-1}, respectively, using $3 \times SD_b$ / slope and $10 \times SD_b$ / slope ratios, respectively, where SD_b is the standard deviation calculated from the ten background current values (blank measurements), determined according to the IUPAC recommendations.[46]

Stability studies of the $Cu(phen)_3(TCNQ)_2$/CNT/GCE

The stability of the $Cu(phen)_3(TCNQ)_2$ modified electrode was also checked in the presence of 100 μmol L^{-1} UA performing successive voltammetric measurements in 0.1 mol L^{-1} PBS at pH 7.0. After 150 voltammetric measurements no change was observed in the response of the modified electrode. When the modified electrode was stored at room temperature no significant change in the response was observed in the period of two months.

In order to study the repeatability of the electrode preparation procedure, six independent electrodes were modified with $Cu(phen)_3(TCNQ)_2$/CNT and voltammetric measurements were performed. The RSD values of measured anodic peak currents were 3.5%.

The utilization of the proposed method in biological sample analysis was also investigated by direct analysis of UA in the presence of AD in three different human urine samples. In this sense, 100 μL of the urine sample were added into 5 mL of 0.1 mol L^{-1} PBS (pH 7.5). The results are presented in Table 2. The percentage of the recovery values was calculated by comparing the concentration obtained from the samples with actual and added concentrations (Table 2). The standard addition method was used for testing recovery. The recovery of the spiked samples ranged between 99.00% and 100.34%, indicating that the proposed sensor is effective and can be applied for UA in real samples. It can be clearly observed that there is no

Table 1. Comparison of some characteristics of the different modified electrodes for determination of UA

Electrode	Technique	Linear range / (μmol L^{-1})	Slope / (A mol^{-1} L)	LOD / (μmol L^{-1})	Reference
Nanowires-$LaPO_4$/CPE	DPV	2.7-24.8	0.01	0.9	36
PAH-HCNTs/GCE	DPV	6-65	0.95	1.5	37
GE/Au/GE/CFE	DPV	12.6-413.62	0.1001	12.6	38
RuON/GCE	DPV	3-56.6; 56.6-758.6	0.0091	0.47	39
GEF/CFE	DPV	3.78-183.87	0.038	2	40
ErGO/CFE	DPV	6-899.3	0.0379	2.23	41
Trp-GR/GCE	DPV	10-1000	0.0601	1.24	42
PPy/FCN/Fe	CV	100-5000	0.00446	23	43
PD-Cu^{II}/GCE	DPV	60-1680	0.003	24.6	44
AT-AuNPs/GCE	amperometry	0.03-100	0.0001	0.000076	45
$Cu(phen)_3(TCNQ)_2$/CNT/GCE	DPV	5-2500	0.11	1.05	this work

Nanowires-$LaPO_4$/CPE: carbon paste electrode coated with $LaPO_4$ nanowires; PAH–HCNTs/GCE: glassy carbon electrode modified with helical carbon nanotubes functionalized with poly(allylamine hydrochloride); GE/Au/GE/CFE: layer-by-layer assembly of graphene sheets and gold nanoparticles modified carbon fiber electrode; RuON/GCE: glassy carbon electrode modified with ruthenium oxide nanoparticles; GEF/CFE: carbon fiber electrode modified by graphene flowers; ErGO/CFE: graphene oxide electrodeposited on carbon fiber electrode; Trp-GR/GCE: glassy carbon electrode modified with tryptophan functionalized graphene; PPy/FCN/Fe: polypyrrole films doped by ferrocyanide ions onto iron electrode; PD-Cu^{II}/GCE: glassy carbon electrode modified with copper(II)-polydopamine; AT-AuNPs/GCE: glassy carbon electrode modified with aminotriazole grafted gold nanoparticles films; $Cu(phen)_3(TCNQ)_2$/CNT/GCE: glassy carbon electrode modified with tris(1,10-phenantroline)copper(II) bis(tetracyanoquinodimethanide) adsorbed on multi-walled carbon nanotubes; DPV: differential pulse voltammetry; CV: cyclic voltammetry; LOD: limit of detection.

Table 2. UA quantification obtained using $Cu(phen)_3(TCNQ)_2$/CNT/GCE

Urine sample (n = 5)	UA[a] quantified / (μmol L^{-1})	UA spiked / (μmol L^{-1})	UA expected / (μmol L^{-1})	UA found / (μmol L^{-1})	Recovery / %
A	30.18 (± 0.10)	20.00	50.18	49.86 (± 0.20)	99.36
B	36.76 (± 0.30)	50.00	86.76	85.90 (± 0.50)	99.00
C	45.50 (± 0.05)	100.00	145.50	146.00 (± 0.18)	100.34

[a]Values obtained without considering the dilution factor (50 times) for samples; UA: urate.

influence of the matrices on the developed sensor for the evaluated samples. In this sense, it is clearly demonstrated that $Cu(phen)_3(TCNQ)_2$/CNT/GCE is a feasible, sensitive, stable and good alternative to simultaneous determination of UA in presence of AD and AA.

Conclusions

The CNT were actually functionalized by suggested methodology involving the compound $Cu(phen)_3(TCNQ)_2$. The composite formed showed electrocatalytic behavior regarding AA, AD and UA oxidations by the change in peak current intensities and in the oxidation potentials. Thus, it allowed building an electrochemical sensor able to selectively determine UA in biological samples owing to high sensibility toward its oxidation and the ability to resolve the overlapping responses with AA and AD. The analyses in urine samples demonstrated that this modified electrode can be used for contributing in diagnostic of many diseases related with UA levels in this biological fluid.

Acknowledgements

The authors are grateful to Conselho Nacional de Desenvolvimento Científico e Tecnológico (CNPq), INCTBio, Rede Mineira de Química, and Fundação de Amparo à Pesquisa do Estado do Maranhão (FAPEMA).

References

1. Becker, B. F.; *Free Radical Biol. Med.* **1993**, *14*, 615.
2. Ballesta-Claver, J.; Rodríguez-Gómez, R.; Capitán-Vallvey, L. F.; *Anal. Chim. Acta* **2013**, *770*, 153.
3. Grabowska, I.; Chudy, M.; Dybko, A.; Brzozka, Z.; *Sens. Actuators, B* **2008**, *130*, 508.
4. Mikkelsen, W. M.; Dodge, H. J.; Valkenburg, H.; *Am. J. Med.* **1965**, *39*, 242.
5. Bianchi, R.; Vitali, C.; Clerico, A.; Pilo, A.; Riente, L.; Fusani, L.; Mariani, G.; *Metabolism* **1979**, *28*, 1105.
6. Kaufman, J. M.; Greene, M. L.; Seegmiller, J. E.; *J. Pediatr.* **1968**, *73*, 583.
7. Iranmanesh, F.; Gadri, F.; Bakhshi, H.; Sarhadi, S.; *Zahedan J. Res. Med. Sci*. **2013**, *15*, 6.
8. Andreadou, E.; Nikolaou, C.; Gournaras, F.; Rentzos, M.; Boufidou, F.; Tsoutsou, A.; Zournas, C.; Zissimopoulos, V.; Vassilopoulos, D.; *Clin. Neurol. Neurosurg.* **2009**, *111*, 724.
9. Pormsila, W.; Krähenbühl, S.; Hauser, P.; *Anal. Chim. Acta* **2009**, *636*, 224.
10. Dai, X.; Fang, X.; Zhang, C.; Xu, R.; Xu, B.; *J. Chromatogr. B: Anal. Technol. Biomed. Life Sci.* **2007**, *857*, 287.
11. Murray, R. W.; Ewing, A. G.; Durst, R. A.; *Anal. Chem.* **1987**, *59*, 379A.
12. Capek, I.; *Adv. Colloid Interface Sci.* **2009**, *150*, 63.
13. Murthy, N.; Surya, A.; Anita; *Bioelectrochem. Bioenerg.* **1994**, *33*, 71.
14. Murthy, N.; Surya, A.; Anita; *Biosens. Bioelectron.* **1994**, *9*, 439.
15. Kulys, J.; D'Costa, E. J.; *Biosens. Bioelectron.* **1991**, *6*, 109.
16. Heintz, R. A.; Zhao, H.; Ouyang, X.; Grandinetti, G.; Cowen, J.; Dunbar, K. R.; *Inorg. Chem.* **1999**, *38*, 144.
17. Luz, R. C. S.; Damos, F. S.; Oliveira, A. B.; Beck, J.; Kubota, L. T.; *Sens. Actuators, B* **2006**, *117*, 274.
18. Rotariu, L.; Zamfir, L.-G.; Bala, C.; *Anal. Chim. Acta* **2012**, *748*, 81.
19. Ren, L.; Fu, L.; Liu, Y.; Chen, S.; Liu, Z.; *Adv. Mater.* **2009**, *21*, 4742.
20. Melby, L. R.; Harder, R. J.; Hertler, W. R.; Mahler, W.; Benson, R. E.; Mochel, W. E.; *J. Am. Chem. Soc.* **1962**, *84*, 3374.
21. Schwartz, M.; Hatfield, W. E.; *Inorg. Chem.* **1987**, *26*, 2823.
22. Mahajan, M.; Bhargava, S. K.; O'Mullane, A. P.; *RSC Adv.* **2013**, *3*, 4440.
23. Kumar, R. S.; Arunachalam, S.; *Polyhedron* **2007**, *26*, 3255.
24. Raman, N.; Pothiraj, K.; Baskaran, T.; *J. Mol. Struct.* **2011**, *1000*, 135.
25. Harris, A. R.; Neufeld, A. K.; O'Mullane, A. P.; Bond, A. M.; *J. Mater. Chem.* **2006**, *16*, 4397.
26. Bond, A. M.; Fletcher, S.; Symons, P. G.; *Analyst* **1998**, *123*, 1891.
27. Laviron, E.; *J. Electroanal. Chem.* **1979**, *101*, 19.
28. Ju, H.; Shen, C.; *Electroanalysis* **2001**, *13*, 789.
29. Bard, A. J.; Faulkner, L. R.; *Electrochemical Methods: Fundamentals and Applications*, 2nd ed.; John Wiley & Sons: New York, 2001.
30. Wang, J.; *Analytical Electrochemistry*, 2nd ed.; John Wiley & Sons: New York, 2000.
31. Kerner, Z.; Pajkossy, T.; *Electrochim. Acta* **2000**, *46*, 207.
32. Lehman, J. H.; Terrones, M.; Mansfield, E.; Hurst, K. E.; Meunier, V.; *Carbon* **2011**, *49*, 2581.
33. Brett, C. M. A.; Brett, A. M. O.; *Electrochemistry: Principles, Methods, and Applications*; Oxford University Press: Oxford, 1993.
34. Wang, G.; Meng, J.; Liu, H.; Jiao, S.; Zhang, W.; Chen, D.; Fang, B.; *Electrochim. Acta* **2008**, *53*, 2837.
35. Ardakani, M. M.; Akrami, Z.; Kazemian, H.; Zare, H. R.; *J. Electroanal. Chem.* **2006**, *586*, 31.
36. Zhou, Y.; Zhang, H.; Xie, H.; Chen, B.; Zhang, L.; Zheng, X.; Jia, P.; *Electrochim. Acta* **2012**, *75*, 360.
37. Cui, R.; Wang, X.; Zhang, G.; Wang, C.; *Sens. Actuators, B* **2012**, *161*, 1139.
38. Du, J.; Yue, R.; Ren, F.; Yao, Z.; Jiang, F.; Yang, P.; Du, Y.; *Gold Bull.* **2013**, *46*, 137.

39. Zare, H. R.; Ghanbari, Z.; Nasirizadeh, N.; Benvidi, A.; *C. R. Chim.* **2013**, *16*, 287.
40. Du, J.; Yue, R.; Re, F.; Yao, Z.; Jiang, F.; Yang, P.; Du, Y.; *Biosens. Bioelectron.* **2014**, *53*, 220.
41. Yang, B.; Wang, H.; Du, J.; Fu, Y.; Yang, P.; Du, Y.; *Colloids Surf., A* **2014**, *456*, 146.
42. Lian, Q.; He, Z.; He, Q.; Luo, A.; Yan, K.; Zhang, D.; Lu, X.; Zhou, X.; *Anal. Chim. Acta* **2014**, *823*, 32.
43. Oukil, D.; Benhaddad, L.; Aitout, R.; Makhloufi, L.; Pillier, F.; Saidani, B.; *Sens. Actuators, B* **2014**, *204*, 203.
44. Huang, L.; Jiao, S.; Li, M.; *Electrochim. Acta* **2014**, *121*, 233.
45. Kesavan, S.; John, S. A.; *Sens. Actuators, B* **2014**, *205*, 352.
46. Analytical Methods Committee; *Analyst* **1987**, *112*, 199.

Submitted: May 14, 2015
Published online: July 24, 2015

FAPESP has sponsored the publication of this article.